STRUCTURE AND THERMAL BEHAVIOR OF TKX-50

Michael Herrmann and Ulrich Förter-Barth

Fraunhofer Institut für Chemische Technologie ICT, D-76327 Pfinztal, Germany
e-mail to michael.herrmann@ict.fraunhofer.de

ABSTRACT

The crystal structure and thermal behavior of TKX-50 has been investigated by means of temperature resolved X-ray diffraction. The energetic material is synthesized at the Fraunhofer ICT and its crystal structure was identified using Rietveld-analysis and reported structure data. Monitoring refined crystal data versus temperature revealed a highly anisotropic expansion behavior connected to a layer structure, but no phase transitions were found between –80 °C and 200 °C. Besides, analysis of anisotropic diffraction peaks broadening gives rise to the hypothesis that the layer structure supports a low sensitivity of TKX-50 without impact to mechanical properties (as found in ADN).

INTRODUCTION

TKX-50 ($C_2H_8N_{10}O_4$, dihydroxylammonium 5,5′-bistetrazole-1,1’-diolate) is a promising, powerful new energetic material. It is easily prepared, insensitive, lowly toxic, and proposed to replace RDX [1-3]. For testing its application possibilities in high explosives, 2 kg TKX-50 were synthesized at the Fraunhofer ICT, the compatibilities with HTPB, Paraffin, wax, GAP, hexogen, aluminum and isocyanates were verified, TKX-50/paraffin wax/graphite charges were pressed, and the charges were characterized in detonation tests [4]. Besides, investigations of the crystal and microstructure by means of powder X-ray diffraction were started in order to characterize the product and determine its thermal behavior.

CRYSTAL STRUCTURE AND THERMAL BEHAVIOR

The crystal structure and thermal behavior of TKX-50 was reported by Fisher et al. [1] in 2012. The structure was investigated by means of X-ray diffraction, and data is deposited at the Cambridge Crystallographic Data Centre [5] e. g. under CCDC 872231 and 872232 for

100 and 298K, respectively. TKX-50 crystallizes in the monoclinic space group $P2_1/c$ with two anion–cation moieties in the unit cell and with a density of 1.877 g cm^{-3} at 298K. Applying DSC the authors did not find any hints to phase transitions up to 222 °C [1]. In contradiction, Lu et al. [6] reported a solid–solid phase transition to a metastable phase (Meta-TKX-50) at about 180 °C, detected with Raman spectroscopy and TGA–DSC. The authors conclude Meta-TKX-50 is formed by the rotation of NH_3OH^+ with 3% volume expansion, a crystal symmetry reduction from $P2_1/c$ to $P\bar{1}$, and a slight change of specific heat capacity, the last being the main reason that the phase transition was overlooked in past measurements. Temperature resolved powder XRD measurements performed by Jia et al. [7] revealed anisotropic thermal expansion of TKX-50 with a negative thermal expansion of the a-axis, which the authors attributed to the distortion of the six-membered ring resulting in H-transfer between the cation and di-anion. Besides, changes in diffraction patterns were monitored with *in situ* isothermal X-ray diffraction, when the substances were monitored up to 6 h at temperatures between 190 and 198 °C. The authors speculated that primary decomposition of TKX-50 occurred with an emerging intermediate product (presumably ABTOX), but no crystalline transition occurred. The structural response of TKX-50 under high pressure up to 10 GPa was examined by Dreger et al. [8] by means of synchrotron single-crystal X-ray diffraction. Investigations revealed a highly anisotropic compression and significantly lower volume compressibility than currently known energetic crystals. Additionally, the experimental data revealed an anomalous compression with even an expansion of the unit cell parameter *a* axis upon compression to ~3 GPa. The authors concluded that the structural stability of TKX-50 is controlled by strong and highly anisotropic intermolecular interactions, and these may contribute to its shock insensitivity.

EXPERIMENTAL

Samples were measured with a Bragg-Brentano diffractometer, D8 Advance from Bruker AXS, equipped with copper tube, Ni filter, two 2.5° Soller collimators, variable V6 divergence slit, a temperature device from MRI, and a silicon strip detector (LynxEye) with 3 °2θ detector opening. Diffraction patterns were monitored between 12 and 50 °2θ with 0.05 °2θ step width and three seconds counting time per step. Temperatures were hold constant, while measuring diffraction patterns, and increased linearly between the measurements with the temperature program 20°C /–80°C /200°C/RT with 20°C steps. Additionally, room temperature measurements were performed with standard sample holder

and anti-scatter aperture between 10 and 60 °2θ with 0.02 °2θ step width. The diffraction patterns were evaluated by means of Rietveld-analysis [9] using the program TOPAS from Bruker AXS [10] and the crystal structure data reported by Fischer et al. [1]. In a further evaluation step, the anisotropic diffraction peak broadening due to small crystallites and/or microstrain was characterized by means of so called Williamson-Hall plots [11, 12]. Therefore, reciprocal peak widths $\beta^*=\beta/\lambda \cos\theta$ are plotted versus reciprocal lattice distances $d^*=2/\lambda \sin\theta$, where β, d, 2θ and λ are the diffraction line width, lattice distance, diffraction angle and the wavelength of the radiation.

RESULTS

Crystal Structure

Figure 1 depicts three elementary cells of TKX-50 viewed along the z-axis, which was generated using the crystal data reported by Fischer et al. [1]. The ions seem to arrange within a layer parallel to the (010) plane (horizontally), which becomes more obvious in the view in Figure 2, where the structure was slightly turned around the y-axis.

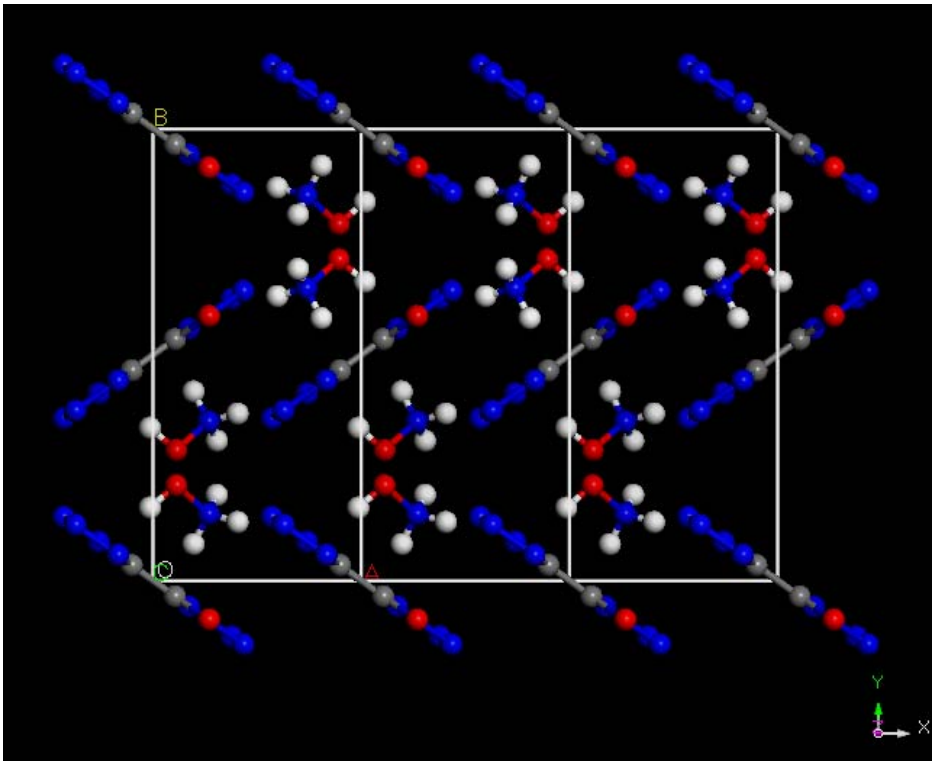

Figure 1 Schematic drawing of TKX-50 with three elementary cells and the arrangement of the cations and anions. The drawing is based on the crystal structure data reported by Fischer et al. [1]; view along the z axis.

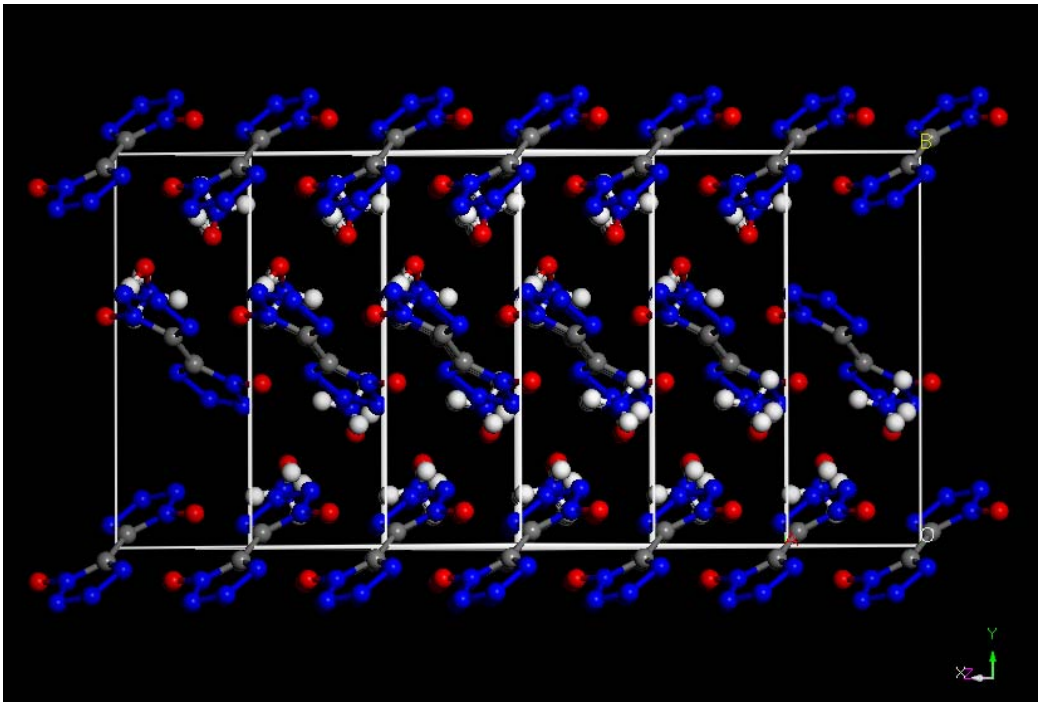

Figure 2 Schematic drawing of TKX-50. Molecules (ions) form layers with (010) orientation.

Our first X-ray diffraction measurements with untreated samples (as synthesized) identified the expected crystal structure, by comparison with calculated patterns of the crystal structure data of CCDC 872232 (298K), but yielded strongly enhanced intensities of the reflection (020), (040) and (060). The differences represent a preferred orientation of crystals, which is typical e. g. for platelets that orientate parallel to the flat sample surfaces during its preparation. Comparing the experimentally found preferred orientation to the crystal structure model in Figure 2, it seems that with a fast growth along (010) layers during the crystallization of TKX-50, and perpendicular to the layers slow growing (010) crystal faces result in a platelet-shaped crystal habit. However, in order to reduce effects of a preferred orientation, samples of TKX-50 were ground for the subsequent investigations.

Moderate Rietveld fits were achieved with the measurements of the ground samples (e. g. Figure 3), but still with some differences at the peaks (020) and (040) at 15.13 and 30.52°2θ and a slight misfit of the peak (031) at 26.62°2θ, resulting in a weighted pattern error of 18.2 and 19.9, when using CCDC 872231 and 872232, respectively. Refined lattice parameters were a = 5.439, b = 11.720, c = 6.546 Å, β = 95.09° and crystal density was found at 1.887 g cm^{-3}, which is slightly higher than the reference value of 1.877 g cm^{-3} given in CCDC 872232. The results are summarized and compared to the reference data in Table 1.

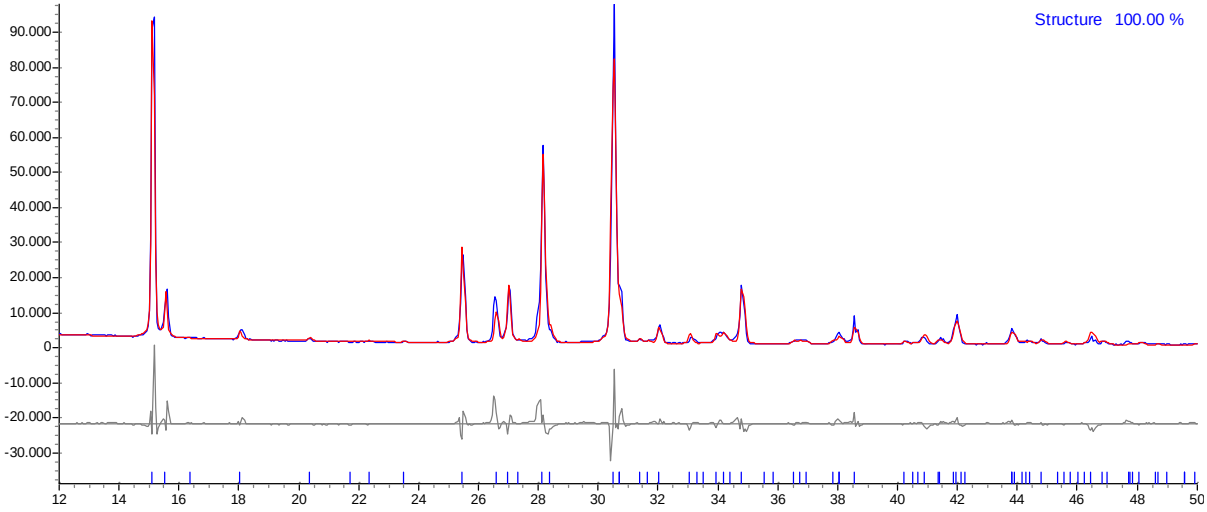

Figure 3 X-ray diffraction pattern of TKX-50 (blue), calculated and fitted pattern (red), differences (grey) and position marker of the calculated structure (blue).

Table 1 Crystal structure data of TKX-50 as reported and measured at the Fraunhofer ICT.

		CCDC 872231	CCDC 872232	FhG ICT
Temperature	[K]	100(2)	298	RT
Lattice parameters				
a	[Å]	5.4872(8)	5.4408(6)	5.439
b	[Å]	11.5472(15)	11.7514(13)	11.720
c	[Å]	6.4833(9)	6.5612(9)	6.546
β	[°]	95.402(12)	95.071(11)	95.09
Cell volume	[Å^3]	408.97(10)	417.86(9)	415.66
Density	[g cm^{-3}]	1.918	1.877	1.887
Rwp				18.2

Thermal behavior of TKX-50

The waterfall plot in Figure 4 depicts diffraction patterns of TKX-50 between 14 and 36 °2θ. It was measured with the temperature program 20 °C (bottom)/–80 °C/200 °C with 20 °C step width and a final measurement at room temperature (top). Peak shifting in the plot represents the thermal expansion/contraction of the crystal structure – a shift to the left correlates to expansion and vice versa. At the seventh pattern (from bottom) shifting changed the direction due to the switching from cooling to heating of the temperature program at –80 °C. Changes between the second last and the last pattern stem from cooling from 200 °C to room temperature. A phase transition, which would be identified by spontaneously changing and emerging new peaks, was not detected.

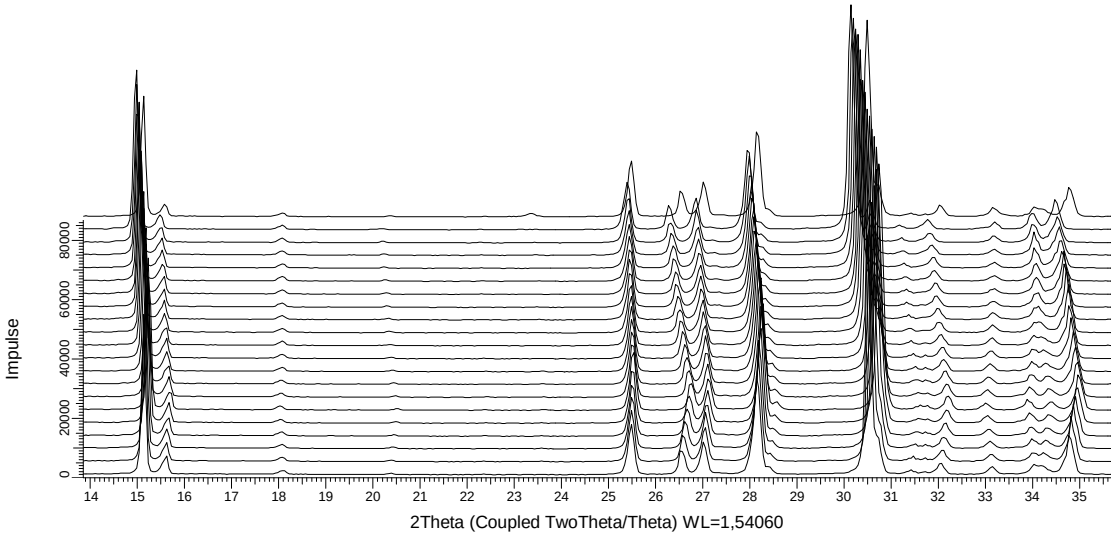

Figure 4 Waterfall plot section of X-ray diffraction measurements of TKX-50. Temperature program 20/–80/200 °C/RT with 20 °C steps (bottom to top).

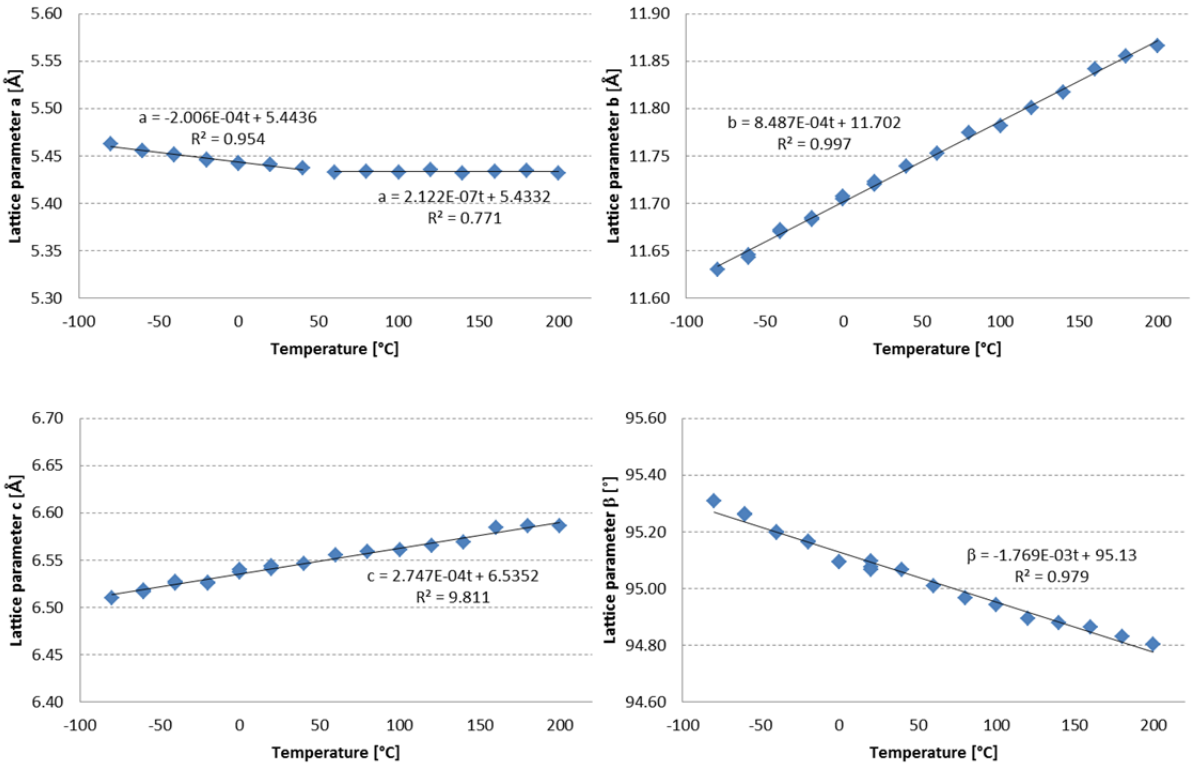

Figure 5 Lattice parameters a, b, c and β of TKX-50 monitored during temperature cycling between –80 and 200 °C.

The crystal structure parameters of TKX-50 are plotted in the Figures 5 and 6 versus temperature and deduced coefficients of thermal expansion (CTEs) are summarized in Table 2. The TKX-50 structure expands anisotropically with a strong thermally induced

expansion of the lattice parameter *b* (7.242 10^{-5} K^{-1}, relative CTE), a medium expansion of *c* (4.197 10^{-5} K^{-1}) versus a slightly contracting lattice parameter *a* (–1.734 10^{-5} K^{-1}). The curve of parameter *a* shows a slight bent at 50 °C; separately evaluated CTEs of the left and right branch are also given in Table 2. Obviously, the values obtained in our investigations are larger by about one order compared to those reported by Jia et al. [7], but with a similar anisotropic behavior. Remark: In the paper of Jia et al. the plot of the normalized unit cell parameters vs. temperature in Figure 3 seems to yield expansion coefficients, which are in the same order as those of our work.

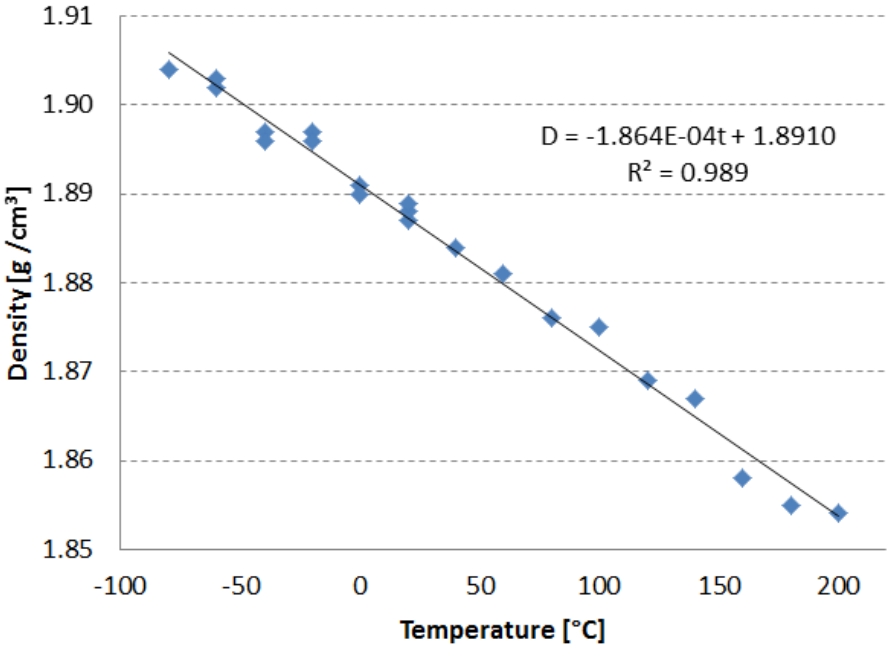

Figure 6 Density of TKX-50 monitored during temperature cycling between –80 and 200 °C.

Table 2 Relative linear thermal expansion coefficients of TKX-50.

Lattice parameters	Coefficients of thermal expansion CTEs this work	Jia et al. [7]
a	-1.734 10^{-5} K^{-1}	–1.04635 x 10^{-06}
< 50 °C	-3.689 10^{-5} K^{-1}	
> 50 °C	3.90110^{-8} K^{-1}	
b	7.242 10^{-5} K^{-1}	5.56149 x 10^{-06}
c	4.197 10^{-5} K^{-1}	4.76293 x 10^{-06}
β	9.996 10^{-5} K^{-1}	–1.92479 x 10^{-07}
spec. Vol.	9.878 10^{-5} K^{-1}	2.2973 x 10^{-07}
Density	-1.734 10^{-5} K^{-1}	

CTEs evaluated relative to the primary value at 20 °C

Anisotropic peak broadening

The reciprocal peak widths β* of TKX-40 are plotted versus reciprocal lattice distances d* in the Williamson-Hall plot in Figure 7. As geometric broadening of the measuring system has not been subtracted beforehand, the results are evaluated in a relative way. For interpretation of the plot the following properties of the Williamson-Hall- plot are considered. Provided that crystallite size or microstrain would be isotropic and no strain broadening occurred, the β*-values would lie on a horizontal line with an intercept at the inverse of the mean linear crystallite size t. In the same case but without size broadening the values would lie on a straight line through the origin with the integral breadth ξ of the strain contribution as slope. However, particle size and strain broadening both can be present and be anisotropic with diffraction order, which results in significant deviations/fluctuations in the Williamson-Hall plots. A straightforward solution can be to use the same set of reflection planes with several orders of reflection [13].

A variety of energetic materials have been investigated with this method at the Fraunhofer ICT, amongst them HMX, RDX, CL-20, FOX-7, FOX-12 and ADN [14-16], and the current results of TKX-50 are discussed in this context. The indexed Williamson-Hall plot of TKX-50 is depicted in Figure 7. The plot shows a wide spreading (wedge-like) distribution of a highly anisotropic structure and reveale one pair of indexed peaks (020)(040) that belong to the same set of reflections. These peaks represent lattice planes parallel to the layers shown in Figure 3. As the data points of these peaks arrange at the bottom of the distribution in the Williamson-Hall plot with comparably low slope of an assumed intersecting straight line, it was concluded that the layering in TKX-50 is not affected by micro strain or defects such as stacking faults. A comparable high broadening was measured for the reflections (110) and (021), but no layer formation was observed parallel to the related lattice planes of the crystal structure. Layer structures were also found in FOX-7 and ADN, where the layers seem to be responsible for the low sensitivity of FOX-7, but are connected to mechanical and thermal stability problems in ADN. In the latter case, analysis of diffraction peak broadening revealed high micro strain related to the layer formation (also along (010) planes), which leads to mechanical instabilities [17]. As this is not the case in TKX-50, the layer structure may support a low sensitivity of the energetic material without impact to its mechanical properties.

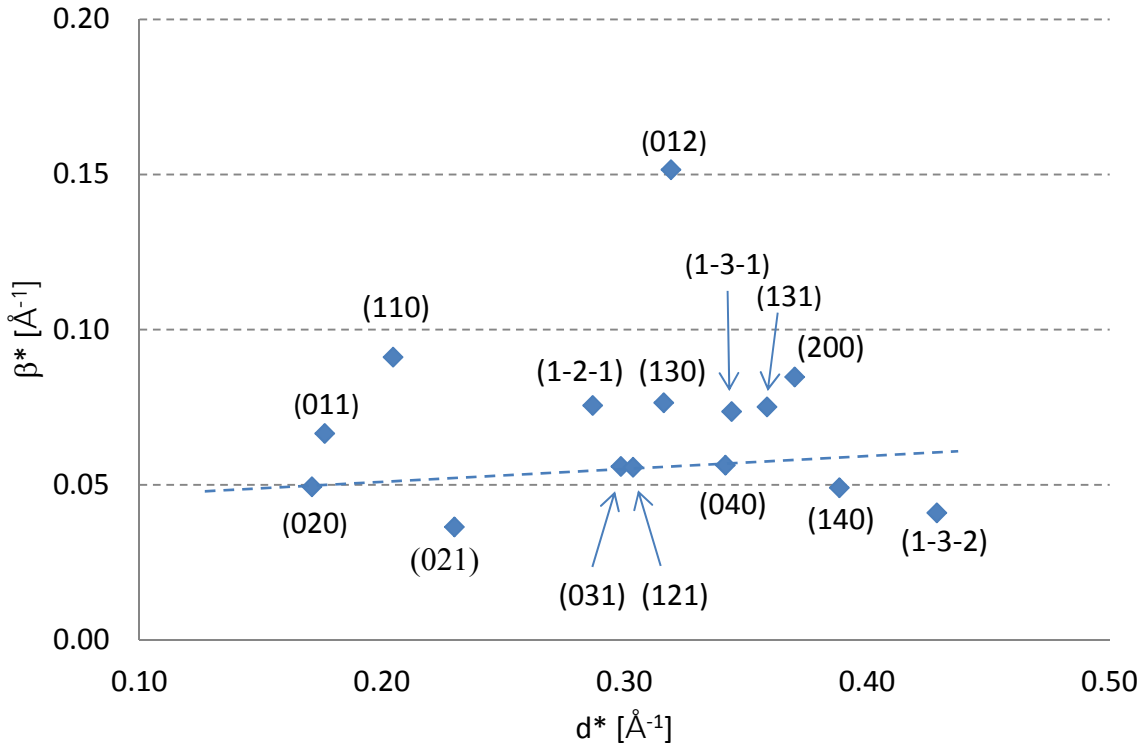

Figure 7 Indexed Williamson-Hall plot of the peak broadening of TKX-50.

Data from measurements at room temperature.

ABBREVIATIONS

ADN	Ammonium dinitramide
CCDC	Cambridge Crystallographic Data Centre
CL-20	Hexanitrohexaazaisowurtzitane
CSD	Cambridge Structural Database
CTEs	Coefficients of thermal expansion
FOX-12	Guarnyl ureadinitramide
FOX-7	1,1-Diamino-2,2-dinitroethylene
GAP	Glycidyl azide polymer
HMX	Cyclotetramethylene tetranitramine, high explosive
ICT	Fraunhofer Institut für Chemische Technologie, Pfinztal, Germany
RDX	Cyclotrimethylene trinitramine, high explosive
TGA–DSC	thermogravimetry–differential scanning calorimetry
TKX-50	Dihydroxylammonium 5,5′-bistetrazole-1,1′-diolate
TRXRD	Temperature resolved X-ray diffraction
XRD	X-ray diffraction

REFERENCES

1. Fischer, N., et al., Pushing the limits of energetic materials – the synthesis and characterization of dihydroxylammonium 5,5′-bistetrazole-1,1′-diolate. Journal of Materials Chemistry, 2012. 22(38).
2. Klapötke, T.M., et al., Determination of the Initiating Capability of Detonators Containing TKX-50, MAD-X1, PETNC, DAAF, RDX, HMX or PETN as a Base Charge, by Underwater Explosion Test. Propellants Explos. Pyrotech., 2016. 41(1): p. 92-97.
3. Witkowski, T.G., Synthesis, Characterization and Testing of Potential Energetic Materials. 2017: Ludwig-Maximilians-Universität, München.
4. Gerber, P., Properties of Explosive Charges based on TKX-50, in 16th International Detonation Symposium. 2018: Cambridge, MD, USA.
5. The Cambridge Structural Database (CSD). [cited 2018; Available from: https://www.ccdc.cam.ac.uk/.
6. Lu, Z., et al., Heat-Induced Solid–Solid Phase Transformation of TKX-50. The Journal of Physical Chemistry C, 2017. 121(15): p. 8262-8271.
7. Jia, J., et al., Crystal structure transformation and step-by-step thermal decomposition behavior of dihydroxylammonium 5,5′-bistetrazole-1,1′-diolate. RSC Adv., 2017. 7(77): p. 49105-49113.
8. Dreger, Z.A., et al., High-Pressure Structural Response of an Insensitive Energetic Crystal: Dihydroxylammonium 5,5′-Bistetrazole-1,1′-diolate (TKX-50). The Journal of Physical Chemistry C, 2017. 121(10): p. 5761-5767.
9. Young, R.A., ed. The Rietveld Method, International Union of Crystallography. ed. I.U.o. Crystallography. 1995, Oxford University Press: New York, USA.
10. DIFFRACplus TOPAS, TOPAS 4.2, B.A. GmbH, Editor. 2009: Karlsruhe, Germany.
11. Williamson, G.K. and W.H. Hall, X-ray line broadening from filed aluminium and wolfram. Acta Metall., 1954. 1: p. 22-31.
12. Langford, J.I., Line Profile and Sample Microstructure, in Industrial Application of X-Ray Diffraction, F.H. Chung and D.K. Smith, Editors. 2000, Marcel Dekker, Inc.: New York.
13. Ungar, T., Warren-Averbach Applications, in Industrial Application of X-Ray Diffraction, F.H. Chung and D.K. Smith, Editors. 2000, Marcel Dekker, Inc.: New York.
14. Herrmann, M., U. Förter-Barth, and P.B. Kempa, Size/stain diffraction peak broadening of the energetic materials HMX, CL-20 and FOX-12. Int. Annu. Conf. ICT, 2009. 40th(Energetic Materials): p. 32/1-32/11.
15. Herrmann, M., U. Förter-Barth, and P.B. Kempa, Size/strain diffraction peak broadening of the energetic materials FOX-7, RDX and ADN. Cent. Eur. J. Energ. Mater., 2009. 6(2): p. 183-193.
16. Herrmann, M., U. Förter-Barth, and P.B. Kempa, Size/strain Diffraction Peak Broadening of the Energetic Materials HMX, CL-20 and FOX-12, in 40th Int. Annu. Conference of Fraunhofer ICT. 2009. p. 32.1–11.
17. Herrmann, M., et al., Thermal Behavior of ADN and ADN-Prills – Crystal and Micro Structure – Part II, in 49th Int. Annu. Conf. of the Fraunhofer ICT. 2018, Fraunhofer ICT: Karlsruhe, Germany. p. 23.1–11.